NAVAL FACILITIES ENGINEERING SERVICE CENTER
Port Hueneme, California 93043-4328

Contract Report
CR 95.002

A NEW METHODOLOGY FOR THE NUMERICAL SIMULATION OF STRAIN SOFTENING IN INELASTIC SOLIDS

An Investigation Conducted by:

J.C. Simo
Department of Mechanical Engineering
Stanford University
Stanford, CA 94305

DTIC
ELECTE
FEB 02 1995
S
G
D

December 1994

19950131 077

ABSTRACT: This document summarizes the work performed by the author and associates at Stanford on a new approach to the analysis and simulation of localization arising in inelastic solids that exhibit strain-softening response. In addition, the document describes new results pertaining to the extension of these ideas to the finite deformation regime. Such an extension will be exploited numerically in follow-up publications. The techniques described in this document lead to the systematic construction of numerical methods that completely eliminate the strong mesh dependence exhibited by conventional treatments of the problem.
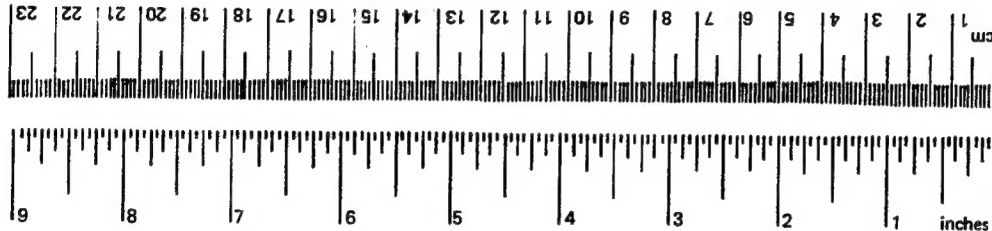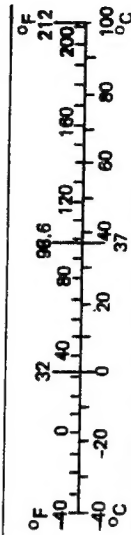
METRIC CONVERSION FACTORS

Approximate Conversions to Metric Measures

Symbol	When You Know	Multiply by	To Find	Symbol
		LENGTH		
in	inches	*2.5	centimeters	cm
ft	feet	30	centimeters	cm
yd	yards	0.9	meters	m
mi	miles	1.6	kilometers	km
		AREA		
in²	square inches	6.5	square centimeters	cm²
ft²	square feet	0.09	square meters	m²
yd²	square yards	0.8	square meters	m²
mi²	square miles	2.6	square kilometers	km²
	acres	0.4	hectares	ha
		MASS (weight)		
oz	ounces	28	grams	g
lb	pounds	0.45	kilograms	kg
	short tons (2,000 lb)	0.9	tonnes	t
		VOLUME		
tsp	teaspoons	5	milliliters	ml
Tbsp	tablespoons	15	milliliters	ml
fl oz	fluid ounces	30	milliliters	ml
c	cups	0.24	liters	l
pt	pints	0.47	liters	l
qt	quarts	0.95	liters	l
gal	gallons	3.8	liters	l
ft³	cubic feet	0.03	cubic meters	m³
yd³	cubic yards	0.76	cubic meters	m³
		TEMPERATURE (exact)		
°F	Fahrenheit temperature	5/9 (after subtracting 32)	Celsius temperature	°C

*1 in = 2.54 (exactly). For other exact conversions and more detailed tables, see NBS Misc. Publ. 286, Units of Weights and Measures, Price $2.25, SD Catalog No. C13.10:286.

Approximate Conversions from Metric Measures

Symbol	When You Know	Multiply by	To Find	Symbol
		LENGTH		
mm	millimeters	0.04	inches	in
cm	centimeters	0.4	inches	in
m	meters	3.3	feet	ft
m	meters	1.1	yards	yd
km	kilometers	0.6	miles	mi
		AREA		
cm²	square centimeters	0.16	square inches	in²
m²	square meters	1.2	square yards	yd²
km²	square kilometers	0.4	square miles	mi²
ha	hectares (10,000 m²)	2.5	acres	
		MASS (weight)		
g	grams	0.035	ounces	oz
kg	kilograms	2.2	pounds	lb
t	tonnes (1,000 kg)	1.1	short tons	
		VOLUME		
ml	milliliters	0.03	fluid ounces	fl oz
l	liters	2.1	pints	pt
l	liters	1.06	quarts	qt
l	liters	0.26	gallons	gal
m³	cubic meters	35	cubic feet	ft³
m³	cubic meters	1.3	cubic yards	yd³
		TEMPERATURE (exact)		
°C	Celsius temperature	9/5 (then add 32)	Fahrenheit temperature	°F

°F -40   0   32   40   80   98.6   120   160   212   °F
°C -40 -20   0   20   37   40   60   80   100   °C

REPORT DOCUMENTATION PAGE

Public reporting burden for this collection of information is estimated to average 1 hour per response, including the time for reviewing instructions, searching existing data sources, gathering and maintaining the data needed, and completing and reviewing the collection of information. Send comments regarding this burden estimate or any other aspect of this collection information, including suggestions for reducing this burden, to Washington Headquarters Services, Directorate for Information and Reports, 1215 Jefferson Davis Highway, Suite 1204, Arlington, VA 22202-4302, and to the Office of Management and Budget, Paperwork Reduction Project (0704-0188), Washington, DC 20503.

1. AGENCY USE ONLY *(Leave blank)*	2. REPORT DATE	3. REPORT TYPE AND DATES COVERED
	December 1994	Final; Oct 1992 - September 1994

4. TITLE AND SUBTITLE
A NEW METHODOLOGY FOR THE NUMERICAL SIMULATION OF STRAIN SOFTENING IN INELASTIC SOLIDS

5. FUNDING NUMBERS

C - N47408-91-C-1217
PE - 61153N
WU - DN666342

6. AUTHOR(S)

Juan C. Simo

7. PERFORMING ORGANIZATION NAME(S) AND ADDRESSE(S)
Division of Applied Mechanics
Department of Mechanical Engineering
Stanford University
Stanford, CA 94305

8. PERFORMING ORGANIZATION REPORT NUMBER

CR 95-002

9. SPONSORING/MONITORING AGENCY NAME(S) AND ADDRESSES
Office of Naval Research / Naval Facilities Engineering
Arlington, VA 22170-5000   Service Center
560 Center Drive
Port Hueneme, CA 93043-4328

10. SPONSORING/MONITORING AGENCY REPORT NUMBER

11. SUPPLEMENTARY NOTES

12a. DISTRIBUTION/AVAILABILITY STATEMENT

Approved for public release; distribution is unlimited.

12b. DISTRIBUTION CODE

13. ABSTRACT *(Maximum 200 words)*

This document summarizes the work performed by the author and associates at Stanford on a new approach to the analysis and simulation of localization arising in inelastic solids that exhibit strain-softening response. In addition, the document describes new results pertaining to the extension of these ideas to the finite deformation regime. Such an extension will be exploited numerically in follow-up publications. The techniques described in this document lead to the systematic construction of numerical methods that completely eliminate the strong mesh dependence exhibited by conventional treatments of the problem.

14. SUBJECT TERMS
Finite element analysis, localization, strain softening, finite deformations, inelastic solids, mesh dependence

15. NUMBER OF PAGES
25

16. PRICE CODE

17. SECURITY CLASSIFICATION OF REPORT	18. SECURITY CLASSIFICATION OF THIS PAGE	19. SECURITY CLASSIFICATION OF ABSTRACT	20. LIMITATION OF ABSTRACT
Unclassified	Unclassified	Unclassified	UL

A NEW METHODOLOGY FOR THE NUMERICAL SIMULATION OF STRAIN SOFTENING IN INELASTIC SOLIDS

J. C. SIMO
Division of Applied Mechanics
Department of Mechanical Engineering
Stanford University, Stanford, CA 94305

Contents

A NEW METHODOLOGY FOR THE NUMERICAL SIMULATION OF STRAIN SOFTENING IN INELASTIC SOLIDS

J. C. SIMO
Division of Applied Mechanics
Department of Mechanical Engineering
Stanford University, Stanford, CA 94305

Abstract

This document summarizes the work performed by the author and his associates at Stanford on a new approach to the analysis and simulation of localization arising in inelastic solids that exhibit strain-softening response. In addition, the document describes new results pertaining to the extension of these ideas to the finite deformation regime. Such an extension will be exploited numerically in follow-up publications. The techniques described below lead to the systematic construction of numerical methods that completely eliminate the strong mesh dependence exhibited by conventional treatments of the problem.

1. Introduction.

In a recent paper Simo, Oliver & Armero [1993] identified key qualitative features exhibited by the response of rate-independent inelastic solids in the presence of strain softening and demonstrated that these features are consistent with solutions possessing a *discontinuous* displacement field in the (quasi-static) rate-independent theory. The analysis performed in this reference for the general three-dimensional problem shows that strong discontinuities (i.e., jumps in the displacement field) are consistent with rate-independent softening response in the isothermal quasi-static regime, provided that the *softening modulus is re-interpreted in a distributional sense.* In particular, for linear softening the inverse of the plastic softening modulus becomes a constant times a delta-function localized at the discontinuity if the problem is to remain mathematically well-posed. In a subsequent paper, Oliver & Simo [1994] extended the preceding analysis to a widely used class of isotropic damage models and showed that the same conclusions remain valid. In particular, we have:

i. The distributional re-interpretation of the softening law leads to a compelling re-interpretation of the softening modulus, related to the fracture energy-released rate in the solid.

ii. Displacement solutions in the presence of strain-softening necessarily yield *discontinuous* displacement fields and, therefore, strain fields which exhibit delta-measures.

iii. Any numerical methods suitable for strain localization must be able to reproduce strain fields with delta-measure. This requirement together with condition **i.** yield numerical solutions that exhibit no mesh-dependence whatsoever.

Strong discontinuities are understood in this work in the sense of solutions exhibiting jumps in the displacement/velocity field across material surfaces (or sets of zero measure). The displacement gradients on both sides of the surface of discontinuity then differ by a bounded measure (a delta-function) while the traction vector remains continuous. The classical example afforded by the slip-lines of rigid plasticity, i.e., bands of *zero thickness* and localized plastic deformation. By contrast, solutions exhibiting *weak* discontinuities remain continuous, while the displacement gradient (not the displacement itself) experiences a jump across the surface of discontinuity. A typical example is provided by the weak shocks observed in elastic materials exhibiting phase transitions. In spite of some confusion in the literature, the numerical analysis issues involved in the simulation of weak shock are significantly different from those arising in the simulation of strong shocks. The former case is treated in reference Mamiya & Simo [1994].

A number of numerical techniques have been proposed in an effort to achieve high resolution of strong discontinuities, the typical example being the discontinuous Galerkin finite element method. Unfortunately, these techniques are often cumbersome to implement, rather expensive, and do not fit the framework for developing high resolution schemes for sharp shock capturing. In Simo, Oliver & Armero [1993] and Simo & Oliver [1994], we have shown that the *Assumed Enhanced Strain* (AES) method of Simo & Rifai [1990] provides an ideal framework for developing high resolution schemes for sharp shock capturing. The AES methodology has been analyzed from a mathematical point of view in Reddy & Simo [1992] and extended to the finite deformation regime in Simo & Armero [1992] and Simo, Armero & Taylor [1993]. The underlying idea for the problem at hand is to replace the strain field by an enhanced strain field designed to replicate delta-functions within a typical element. The explicit construction is described in detail in Simo & Oliver [1994] within the context of the infinitesimal theory and below for the full finite deformation problem. A similar idea also works for the motion of weak shocks in phase transition problems (see Mamiya & Simo [1994]).

An outline of the rest of this report is as follows. Section 2 generalizes the basic results described in Simo & Oliver [1994] on the kinematics and balance laws for the problems with strong discontinuities to the full finite deformation regime. Section 3 presents completely new results on finite strain plasticity in the presence of strong discontinuities that generalizes to the finite strain regime the techniques described in Simo, Oliver & Armero [1993] and summarized above. Finally, Section 4 describes a new finite element method for the accurate resolution of strong discontinuities that generalizes to the finite strain regime the technique described in Simo & Oliver [1994]. In sharp contrast with recent approaches,

see e.g. Larsson, Runesson & Ottosen [1994], in the techniques developed in the course of this research the shock does not need to coincide with element sides.

As part of the proposed research effort, we have developed new constitutive models for geomaterials in Simo & Meschke [1993]. In addition, a rather attractive material model for plane concrete that incorporates anisotropic damage is presented in Govindjee, Kay & Simo [1994]. Lack of space prevents us to describe in detail these developments. Similarly, no details will be given on either the mathematical analysis of enhanced strain methods presented in Reddy & Simo [1992] or the class of assumed enhanced strain methods described in Simo, Armero & Taylor [1993].

2. Kinematics and Balance Laws in the Presence of shocks.

We summarize below the basic notation employed throughout this work and introduce a fundamental decomposition of the displacement field into a regular part and a discontinuous part. Such a decomposition plays a key role in proposed numerical treatment of the problem. We conclude this section with the statement of the weak form of the equations and a rigorous derivation of the local equilibrium equations.
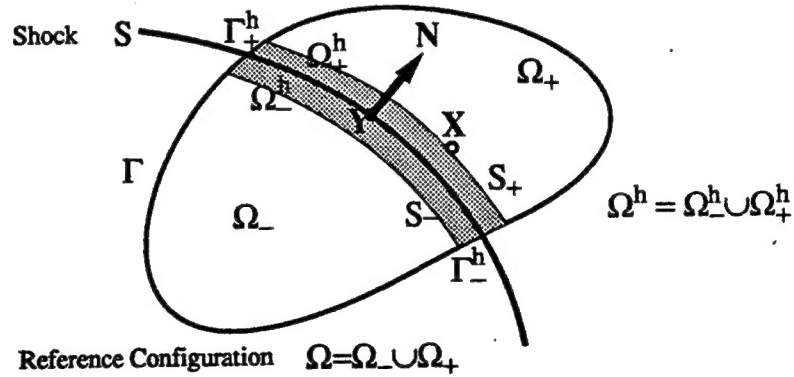
FIGURE 2.1. Material surface S in the domain Ω, with unit normal N : $S \rightarrow S^2$, and normal parameterization $X = Y + \eta N$ with $\eta \in [-h, h]$. The surface S divides both Ω and $\Omega^h \subset \Omega$ into two subdomains labeled $\Omega_\pm$ and $\Omega^h_\pm \subset \Omega_\pm$, respectively.

2.1. Spatially Discontinuous Motions. Basic Notation.

We denote by $\Omega \subset \mathbb{R}^{n_{\dim}}$ the reference configuration of a continuum body with smooth boundary $\partial \Omega$ and particles labeled by $X \in \Omega$. The starting point of the analysis of

solutions exhibiting strain softening is a motion $\varphi : \bar{\Omega} \times \mathsf{I} \to \mathbb{R}^{n_{\dim}}$, which is assumed to experienced a jump discontinuity $[\![\varphi]\!] \neq 0$ on a smooth material surface $\mathcal{S} \subset \Omega$. Here I denotes the time interval of interest. Since $\mathcal{S}$ is a material surface we have $\dot{\mathcal{S}} = 0$. Points in $\mathcal{S}$ are denoted by Y, with the notation indicated in Figure 1 assumed throughout. For simplicity we assume that $\mathcal{S}$ is smooth, with unit normal vector field denoted by $N(Y)$ so that

$$\mathcal{S} = \left\{ Y = \hat{Y}(\xi^1, \xi^2) : \ (\xi^1, \xi^2) \in \mathcal{B} \right\}, \tag{2.1a}$$

where $\hat{Y} : \mathcal{B} \to \Omega$ is a smooth global parametrization. The unit normal field to $\mathcal{S}$ is then given by

$$N = \hat{N}(\xi^1, \xi^2) := \hat{Y}_{,1} \times \hat{Y}_{,2} \ \Big/ \ \| \hat{Y}_{,1} \times \hat{Y}_{,2} \|. \tag{2.1b}$$

A parametrization of $\mathcal{S}$ induces in turn a convenient parameterization valid in a neighborhood $\Omega^h = \mathcal{S} \times (-h, h)$ of $\mathcal{S}$, known as a *normal parametrization* and defined via the formula

$$\hat{X}(\xi^1, \xi^2, \eta) := \hat{Y}(\xi^1, \xi^2) + \eta \, \hat{N}(\xi^1, \xi^2) \quad \text{for} \quad -h \leq \eta \leq h. \tag{2.2}$$

The boundary $\partial \Omega^h$ of the set Ω^h is composed of the surfaces shown in 2.1, so that

$$\partial \Omega^h = \mathcal{S}_-^h \cup \mathcal{S}_+^h \cup \Gamma_-^h \cup \Gamma_+^h, \tag{2.3}$$

where $\Gamma^h = \Gamma_-^h \cup \Gamma_+^h$ is the intersections of $\bar{\Omega}^h$ with the outer boundary $\partial \Omega$ of Ω. Given an arbitrary function $\psi : \bar{\Omega}^h \times \mathsf{I} \to \mathbb{R}$, we let

$$\hat{\psi}(\xi^1, \xi^2, \eta, t) := \psi(\hat{X}(\xi^1, \xi^2, \eta), t). \tag{2.4a}$$

With a slight abuse in notation, we shall use the same symbol to denote both the function ψ and its representative $\hat{\psi}$ defined by (2.4a) in the normal parametrization. In addition, we denote by $\{G^1, G^2, \hat{N}\}$ the basis dual to the curvilinear basis $\{\hat{X}_{,1}, \hat{X}_{,2}, \hat{N}\}$ associated with the normal parametrization, so that $\hat{X}_\alpha \cdot G^\beta = \delta_\alpha^\beta$ for $\alpha, \beta = 1, 2$. It follows that the gradient of ψ can be written as

$$\mathrm{GRAD}[\psi] = \mathrm{GRAD}_{\mathcal{S}}[\psi] + [\partial \psi / \partial \eta] N, \tag{2.4b}$$

where

$$\mathrm{GRAD}_{\mathcal{S}}[\psi] := \sum_{\alpha=1}^{n_{\dim}-1} [\partial \psi / \partial \xi^\alpha] G^\alpha, \tag{2.4c}$$

Clearly, by construction we have $N \cdot \mathrm{GRAD}_{\mathcal{S}}[\psi] = 0$. Finally, the motion $\varphi(X, t)$ is subjected to the usual essential and boundary conditions. Explicitly, we assume that on parts $\Gamma_u \subset \partial \Omega$ and $\Gamma_t \subset \Gamma$ we have

$$\varphi = g \ \text{ on } \ \Gamma_u \times \mathsf{I} \quad \text{and} \quad P\nu = t \ \text{ on } \ \Gamma_t \times \mathsf{I}, \tag{2.5}$$

where g and t are prescribed vector fields on $\partial \Omega$, ν is the unit outward normal field to $\partial \Omega$ and P denotes the *nominal stress* tensor. We assume that $\Gamma_u \cup \Gamma_t = \partial \Omega$ while $\Gamma_u \cap \Gamma_t = \emptyset$.

2.2 Decomposition of the Spatially Discontinuous Motion

The numerical approach described below relies crucially on a decomposition of the motion into a *regular or smooth* part and a *discontinuous* part. The regular part in such a decomposition is assumed to obey the same essential boundary conditions $(2.5)_1$ as the motion. Accordingly, we set

$$\varphi(X,t) = \underbrace{\bar{\varphi}(X,t)}_{\text{Regular Part}} + \underbrace{M_S(X)[\![\varphi]\!](Y,t)}_{\text{Discontinous Part}}, \quad \text{for } (X,t) \in \Omega \times \mathsf{I}. \tag{2.6}$$

Here, $[\![\varphi]\!](Y,t)$ is the jump experience by φ across S defined in the usual fashion, see e.g., Truesdell & Toupin [1960], and $M_S : \bar{\Omega}^h \to \mathbb{R}$ is a prescribed function subject to the following two conditions:

i. The jump across S is $[\![M_S]\!] = 1$.

ii. The support of M_S is $\operatorname{supp}[M_S] = \bar{\Omega}^h$ with $M_S = 0$ on $S_{\pm}^h$.

A convenient expression for the function M_S is obtained by means of the following construction. Relative to a normal parametrization $X = Y + \eta N$ we set

$$M_S(X) = H_S(\eta) - \psi^h(X) \quad \text{where} \quad H_S(\eta) = \begin{cases} 1 & \text{if } \eta > 0, \\ 0 & \text{if } \eta < 0, \end{cases} \tag{2.7}$$

is the Heaviside function. The function ψ^h is smooth and completely arbitrary, except for the following two requirements:

$$\psi^h(X) = 0 \text{ for } X \in \Omega_- \backslash \Omega_-^h \quad \text{and} \quad \psi^h(X) = 1 \text{ for } X \in \Omega_+ \backslash \Omega_+^h. \tag{2.8}$$

The properties of the Heaviside function imply that condition **i** holds for M_S defined by (2.7), while restriction (2.8) ensures that condition **ii** also holds.

REMARK 2.1. For the case $n_{\dim} = 1$ S collapses to a point, say $x = \xi$, and definition (2.7) reduces to $M_S(\eta) = H(\xi + \eta) - \psi^h(\xi + \eta)$. The restriction (2.8) on ψ^h merely becomes

$$\psi^h(\xi + \eta) = 0 \text{ for } \eta \leq -h \quad \text{and} \quad \psi^h(\xi + \eta) = 1 \text{ for } \eta \geq h. \tag{2.9}$$

The derivative of M_S is obviously given by $M_S'(\eta) = \delta_\xi(\xi + \eta) - \psi^{h\prime}(\xi + \eta)$. ∎

For subsequent use, we recall that $\operatorname{GRAD}[H_S] = \delta_S N$ for $n_{\dim} > 1$, where δ_S is the Dirac delta measure on the surface S. Using this elementary result in the theory of distributions, the derivative of the function M_S takes the form

$$\operatorname{GRAD}[M_S] = \delta_S N - \operatorname{GRAD}[\psi^h]. \tag{2.10}$$

We remark that the smoothness restriction on the regular part $\bar{\varphi}$ of the motion is introduced only for simplicity. Continuity of $\bar{\varphi}$ is all that is required for the arguments below to remain valid.

2.3 The Weak and Local Form of the Equilibrium Equations

Again for simplicity, attention will be restricted in the developments below to the quasi-static problem under the assumption of small deformations. Our goal is a careful statement of the local equations of equilibrium for the problem at hand. Our point of departure is the weak form of the equations as defined by the classical principle of virtual work, i.e.,

$$\int_{\Omega} \boldsymbol{P} : \mathrm{GRAD}[\boldsymbol{\eta}] \, d\Omega = \int_{\Omega} \boldsymbol{f} \cdot \boldsymbol{\eta} \, d\Omega + \int_{\Gamma_t} \boldsymbol{t} \cdot \boldsymbol{\eta} \, d\Gamma, \tag{2.11}$$

for all admissible test functions (virtual displacements) $\boldsymbol{\eta} \in \mathcal{V}$, where $\boldsymbol{f}$ stands for the prescribed body force. Consistent with the form (2.6) adopted for the displacement field, the space $\mathcal{V}$ of admissible variations is defined by

$$\mathcal{V} := \left\{ \boldsymbol{\eta} = \bar{\boldsymbol{\eta}} + M_{\mathcal{S}} \boldsymbol{\beta} : \left. \bar{\boldsymbol{\eta}} \right|_{\Gamma_u} = \boldsymbol{0} \quad \text{and} \quad \boldsymbol{\beta} : \mathcal{S} \to \mathbb{R}^{n_{\dim}} \text{ is arbitrary} \right\}, \tag{2.12}$$

where the regular part $\bar{\boldsymbol{\eta}}$ of $\boldsymbol{\eta} \in \mathcal{V}$ is smooth. We have the following result.

LEMMA 2.1. The weak form (2.11) along with (2.12) yield the local equilibrium equation

$$\left. \begin{array}{rcll} \mathrm{DIV}[\boldsymbol{P}] + \boldsymbol{f} &=& \boldsymbol{0} & \text{in} \quad \Omega \backslash \mathcal{S} \times \mathsf{I} \\ \boldsymbol{P}\boldsymbol{\nu} &=& \boldsymbol{t} & \text{on} \quad \Gamma_t \times \mathsf{I} \end{array} \right\} \tag{2.13a}$$

supplemented with the following two conditions:

$$[\![\boldsymbol{P}\boldsymbol{N}]\!] = [\,\boldsymbol{P}_+ - \boldsymbol{P}_-\,]\,\boldsymbol{N} = \boldsymbol{0} \quad \text{and} \quad \boldsymbol{P}_{\mathcal{S}}\,\boldsymbol{N} = \boldsymbol{P}_+\,\boldsymbol{N}. \tag{2.13b}$$

Here $\boldsymbol{P}_{\mathcal{S}}\,\boldsymbol{N}$ denotes the traction vector *acting on the surface* $\mathcal{S}$.

Proof: We proceed in two steps. (i) First, choose *regular* test functions with $\boldsymbol{\beta} \equiv \boldsymbol{0}$, so that $\mathrm{GRAD}[\boldsymbol{\eta}] = \mathrm{GRAD}[\bar{\boldsymbol{\eta}}]$ with $\bar{\boldsymbol{\eta}}$ arbitrary. Integration by parts then yields

$$\int_{\Omega} \boldsymbol{P} : \mathrm{GRAD}[\boldsymbol{\eta}] \, d\Omega = - \int_{\Omega} \bar{\boldsymbol{\eta}} \cdot \mathrm{DIV}[\boldsymbol{P}] \, d\Omega$$
$$+ \int_{\mathcal{S}} \boldsymbol{\eta} \cdot ([\![\boldsymbol{P}]\!]\,\boldsymbol{N}) \cdot d\mathcal{S} + \int_{\Gamma_t} \boldsymbol{\eta} \cdot (\boldsymbol{P}\boldsymbol{N}) \, d\Gamma. \tag{2.14}$$

By inserting (2.14) into (2.11) a standard argument yields (2.13a) and (2.13b)₁.

(ii) Second, choose test functions with the regular part $\bar{\eta} \equiv 0$ and function $M_{\mathcal{S}}$ defined by (2.7). From (2.10) we have

$$\text{GRAD}[\eta] = -\boldsymbol{\beta} \otimes \text{GRAD}[\psi^h] + M_{\mathcal{S}} + \delta_{\mathcal{S}} \boldsymbol{\beta} \otimes \boldsymbol{N} + \text{GRAD}_{\mathcal{S}}[\boldsymbol{\beta}], \tag{2.15}$$

where $\text{GRAD}_{\mathcal{S}}[\boldsymbol{\beta}] = \sum_{\alpha=1}^{n_{\dim}-1} \boldsymbol{\beta}_{,\alpha} \otimes \boldsymbol{G}^{\alpha}$, see (2.4). The contribution of the first term in (2.15) to the weak form (2.11) is evaluated as follows. Integration by parts along with the local equilibrium equation (2.13a)$_1$ gives

$$
\begin{aligned}
\int_{\Omega^h} \boldsymbol{P} : (\boldsymbol{\beta} \otimes \text{GRAD}[\psi^h]) \, d\Omega = \ & \int_{\Omega^h} \text{DIV}[\psi^h \boldsymbol{P} \boldsymbol{\beta}] \, d\Omega \\
& - \int_{\Omega^h} \psi^h \left[\boldsymbol{\beta} \cdot \text{DIV}[\boldsymbol{P}] + \boldsymbol{P} : \text{GRAD}_{\mathcal{S}}[\boldsymbol{\beta}] \right] d\Omega \\
= \ & \int_{\mathcal{S}_+} \psi^h \boldsymbol{\beta} \cdot \boldsymbol{P} \boldsymbol{N} \, d\mathcal{S} - \int_{\mathcal{S}_-} \psi^h \boldsymbol{\beta} \cdot \boldsymbol{P} \boldsymbol{N} \, d\mathcal{S} \\
& - \int_{\mathcal{S}} \psi^h \boldsymbol{\beta} \cdot [\boldsymbol{P}] \boldsymbol{N} \, d\mathcal{S} \\
& + \int_{\Omega^h} \psi^h \left[\boldsymbol{f} \cdot \boldsymbol{\beta} - \boldsymbol{P} : \text{GRAD}_{\mathcal{S}}[\boldsymbol{\beta}] \right] d\Omega.
\end{aligned}
\tag{2.16}
$$

Use of the boundary conditions $\psi^h = 1$ on $\mathcal{S}_+^h$ and $\psi = 0$ on $\mathcal{S}_-^h$, together with the jump condition (2.13b)$_2$ and expression (2.7) for $M_{\mathcal{S}}$, yields

$$
\begin{aligned}
\int_{\Omega^h} \boldsymbol{P} : (\boldsymbol{\beta} \otimes \text{GRAD}[\psi^h]) \, d\Omega = \ & \int_{\mathcal{S}} \boldsymbol{\beta} \cdot \boldsymbol{P} \boldsymbol{N} \, d\mathcal{S} - \int_{\Omega^h} \left[\boldsymbol{f} \cdot \boldsymbol{\beta} - \boldsymbol{P} : \text{GRAD}_{\mathcal{S}}[\boldsymbol{\beta}] \right] M_{\mathcal{S}} \, d\Omega \\
& + \int_{\Omega_+^h} \left[\boldsymbol{f} \cdot \boldsymbol{\beta} - \boldsymbol{P} : \text{GRAD}_{\mathcal{S}}[\boldsymbol{\beta}] \right] d\Omega.
\end{aligned}
\tag{2.17}
$$

Inserting (2.15) into the weak form (2.11) of the equilibrium equations and making use of (2.17) gives the following result:

$$\int_{\mathcal{S}} \boldsymbol{\beta} \cdot \boldsymbol{P}_{\mathcal{S}} \boldsymbol{N} \, d\mathcal{S} - \int_{\mathcal{S}_+^h} \boldsymbol{\beta} \cdot \boldsymbol{P} \boldsymbol{N} \, d\mathcal{S} - \int_{\Omega_+^h} \left[\boldsymbol{f} \cdot \boldsymbol{\beta} - \boldsymbol{P} : \text{GRAD}_{\mathcal{S}}[\boldsymbol{\beta}] \right] d\Omega = 0, \tag{2.18}$$

for any $\boldsymbol{\beta} : \mathcal{S} \to \mathbf{R}^{n_{\dim}}$. The last step in the proof involves the evaluation of the integral involving the term $\boldsymbol{P} : \text{GRAD}_{\mathcal{S}}[\boldsymbol{\beta}] = \boldsymbol{\beta}_{,\alpha} \cdot \boldsymbol{P} \boldsymbol{g}^{\alpha}$. Since in a normal parametrization $\Omega_+^h = \mathcal{S} \times [0, h]$, using integration by parts and the assumption that the lateral boundary $\Gamma^h = \Gamma_+^h \cup \Gamma_-^h$ is traction free it is easily shown that

$$\int_{\Omega_+^h} \boldsymbol{P} : \text{GRAD}_{\mathcal{S}}[\boldsymbol{\beta}] \, d\Omega = - \int_{\Omega_+^h} \boldsymbol{\beta} \cdot \text{DIV}[\boldsymbol{P}] \, d\Omega + \int_{\mathcal{S} \times [0,h]} \boldsymbol{\beta} \cdot (\boldsymbol{P} \boldsymbol{N})_{,\eta} \, d\mathcal{S} d\eta. \tag{2.19}$$

Inserting the local equilibrium equation $(2.13a)_1$ into (2.19) yields

$$-\int_{\Omega^h_+} [\boldsymbol{f} \cdot \boldsymbol{\beta} - \boldsymbol{P} : \mathrm{GRAD}_{\mathcal{S}}[\boldsymbol{\beta}]] \, d\Omega = \int_{\mathcal{S}^h_+} \boldsymbol{\beta} \cdot (\boldsymbol{PN}) \, d\mathcal{S} - \int_{\mathcal{S}} \boldsymbol{\beta} \cdot (\boldsymbol{P}_+\boldsymbol{N}) \, d\mathcal{S}. \qquad (2.20)$$

By combining (2.20) and (2.18) we conclude that the weak form of the equilibrium equations finally reduces to

$$\int_{\mathcal{S}} \boldsymbol{\beta} \cdot [\boldsymbol{P}_{\mathcal{S}}\boldsymbol{N} - \boldsymbol{P}_+\boldsymbol{N}] \, d\mathcal{S}, \quad \forall \boldsymbol{\beta} : \mathcal{S} \rightarrow \mathbb{R}^{n_{\dim}}. \qquad (2.21)$$

A standard argument then yields result $(2.13b)_2$.   ■

REMARK 2.2. Results $(2.13a)$ and $(2.13b)_1$ are classical for problems exhibiting discontinuities. Result $(2.13b)_2$, on the other hand, is non–conventional and arises from the decomposition (2.6) of the displacement field. The different physical significance of these two conditions becomes clear if we replace the shock $\mathcal{S}$ by the neighborhood Ω^h with finite thickness h. Condition $(2.13b)_1$ then becomes a restatement of continuity of the traction vector across the material shock $\mathcal{S}$, in the sense that the traction vectors on $\mathcal{S}^h_+$ and $\mathcal{S}^h_-$ coincide, while condition $(2.13b)_2$ is the assertion that traction vector *on the shock itself* $\mathcal{S}$ equals the traction vector on $\mathcal{S}^h_+$ ahead the shock.   ■

3 Finite Plasticity in the Presence of Softening

Classical rate independent models of plasticity lead to ill–posed initial boundary value problems in the presence of strain–softening (as opposed to strain–hardening) response. This lack of well-posedness manifests itself in a computational setting in a strong–mesh dependence of the numerical solution. Within the scope of the infinitesimal theory, it was shown in Simo, Oliver & Armero [1993] that well–posedness in strain–softening models of rate–independent plasticity is restored if the hardening law is reinterpreted in a distributional sense. Moreover, this reformulation of the Hardening law lends itself to a compelling physical interpretation. The goal of this section is to generalize these results to the full finite deformation theory.

3.1 Deformation Gradients and Spatial Rates of Deformation

The first step in the analysis is to compute the deformation gradient and the associated rates of deformation tensors for a discontinuous motion of the form (2.6). For convenience, $M_{\mathcal{S}}$ is assumed to be given by (2.7). Accordingly, setting

$$\bar{\boldsymbol{F}} := \mathrm{GRAD}[\bar{\varphi}] + M_{\mathcal{S}} \mathrm{GRAD}_{\mathcal{S}} [\![\varphi]\!] - [\![\varphi]\!] \otimes \mathrm{GRAD}[\psi^h], \qquad (3.1)$$

and recalling that $\mathrm{GRAD}[H_\mathcal{S}] = \delta_\mathcal{S} N$, the deformation gradient $F := \mathrm{GRAD}[\varphi]$ can be written as

$$F = \bar{F} + \delta_\mathcal{S}[\![\varphi]\!] \otimes N \quad \text{in } \Omega \times \mathsf{I}. \tag{3.2a}$$

Alternatively, by defining the *material jump* J as

$$J = \bar{F}^{-1}[\![\varphi]\!], \tag{3.3}$$

expression (3.2) for the deformation gradient can be written in the following entirely equivalent form:

$$F = \bar{F} F^* \quad \text{where} \quad F^* := 1 + \delta_\mathcal{S} J \otimes N. \tag{3.2b}$$

This kinematic decomposition, which arises in the present context without any a-priori kinematic assumption, is formally identical to the multiplicative decomposition $F = F^e F^p$ of the deformation gradient postulated at the outset in certain formulations of plasticity, see e.g., Lee [1969], Mandel [1974] and Simo [1992, 1994] among others. For the problem at hand, the elastic part is $F^e = \bar{F}$ while the plastic part becomes $F^p = F^*$. In order to circumvent technical difficulties, the following additional hypothesis is introduced.

ASSUMPTION 3.1. The unit vector N normal to the material discontinuity $\mathcal{S}$ is *orthogonal* to the material jump J, so that the following equivalent conditions are assumed to hold:

$$N \cdot J = 0 \iff n \cdot [\![\varphi]\!] = 0 \quad \text{where} \quad n := \bar{F}^{-T} N. \tag{3.4}$$

It follows from $(3.4)_2$ that n can by interpreted as the vector normal to the surface $\bar{\varphi}(\mathcal{S})$ in the current configuration of the solid. ∎

Expressed in physical terms, condition (3.4) asserts that only *slips* (i.e., jumps $[\![\varphi]\!]$ which are tangential to $\mathcal{S}$) are allowed. Under such a restriction, the inverse of the deformation gradient F^* takes the simple form

$$F^{*-1} = 1 - \delta_\mathcal{S} J \otimes N; \tag{3.5}$$

a result which is immediately verified by a direct computation.

REMARK 3.1. If the normal n to $\bar{\varphi}(\mathcal{S})$ is not orthogonal to the jump $[\![\varphi]\!]$, it is easily verified that expression (3.5) remains formally valid, provided that the delta measure $\delta_\mathcal{S}$ replaced by the factor $[1 - \delta_\mathcal{S}[\![\varphi]\!] \cdot n]^{-1}\delta_\mathcal{S}$. ∎

The next step is to compute the spatial velocity gradients $l := \mathrm{GRAD}[\dot{\varphi}]F^{-1}$ and $\bar{l} := \mathrm{GRAD}[\dot{\bar{\varphi}}]\bar{F}^{-1}$ associated with the motions φ and $\bar{\varphi}$, respectively. A straightforward manipulation then yields the following standard expressions in continuum mechanics:

$$l = \dot{F} F^{-1} \quad \text{and} \quad \bar{l} = \dot{\bar{F}} \bar{F}^{-1}. \tag{3.6}$$

According to the preceding interpretation, we can view l and $\bar{l}$ as the total and the elastic spatial velocity gradients, respectively. The following result determines the plastic velocity gradient.

LEMMA 3.1. The local velocity gradient l^* associated with the part F^* of the deformation gradient obeys the additive decomposition

$$l = \bar{l} + l^* \quad \text{with} \quad l^* := \delta_S \left(L_{\bar{v}}[\![\varphi]\!] \right) \otimes n, \tag{3.7a}$$

and

$$L_{\bar{v}}[\![\varphi]\!] := \frac{\partial [\![\varphi]\!]}{\partial t} - \bar{l}\,[\![\varphi]\!] \quad \text{where} \quad \bar{v} := \frac{\partial \bar{\varphi}}{\partial t} \circ \bar{\varphi}^{-1} \tag{3.7b}$$

is the Lie derivative relative to the spatial velocity field $\bar{v}$.

PROOF. Time differentiation of the relation $F = \bar{F} F^*$ yield, after post-multiplication by F^{-1}, the result

$$l = \bar{l} + \bar{F}\,[L^*]\,\bar{F}^{-1} \quad \text{where} \quad L^* := \frac{\partial F^*}{\partial t} F^{*-1}. \tag{3.8}$$

Now, time differentiation of expression $(3.2b)_2$ and use of result (3.5) yields

$$L^* = \left[\delta_S \dot{J} \otimes N \right] [1 - \delta_S J \otimes N] = \delta_S \dot{J} \otimes N, \tag{3.9}$$

since $N \cdot J = 0$ by assumption (3.4). Therefore, we have

$$\bar{F}\,[L^*]\,\bar{F}^{-1} = \delta_S(\bar{F}\dot{J}) \otimes n = \delta_S L_{\bar{v}}[\![\varphi]\!] \otimes n. \tag{3.10}$$

and the result follows by inserting (3.10) into (3.8). ∎

REMARK 3.2. A standard result in continuum mechanics shows that the Lie derivative $L_{\bar{v}}[\![\varphi]\!]$ is objective. Since the normal n is also objective, it follows that the *full* spatial velocity gradient gradient l^* is objective in the standard sense, i.e.,

$$l^{*+} = Q l^* Q^T \quad \text{if} \quad x \mapsto x^+ := r + Qx, \tag{3.11}$$

for arbitrary translations $r \in \mathbb{R}^3$ and arbitrary rotations $Q \in SO(3)$. On the other hand, only the symmetric parts $d := \mathrm{sym}[l]$ and $\bar{d} := \mathrm{sym}[\bar{l}]$ —the so-called spatial rate of deformation tensors— are objective. An identical result holds for finite deformation multiplicative plasticity, see Simo [1994]. We shall denote by $w := \mathrm{skew}[l]$, $\bar{w} = \mathrm{skew}[\bar{l}]$ and $w^* = \mathrm{skew}[l^*]$ the *spin tensors*. ∎

3.2 Analysis of Discontinuous Solutions. Localization Conditions

Consider next a conventional model of classical rate–independent plasticity with isotropic hardening/softening law expressed in *rate form* via the following constitutive equations:

$$\left. \begin{array}{l} \overset{\triangledown}{\boldsymbol{\tau}} = \mathbf{c}\,[\boldsymbol{l} - \boldsymbol{l}^p] \\[4pt] \boldsymbol{l}^p = \lambda\,\partial_{\boldsymbol{\tau}}\phi(\boldsymbol{\tau}, q) \\[4pt] \dot{\alpha} = \lambda\partial_q\phi(\boldsymbol{\tau}, q) \end{array} \right\} \tag{3.12}$$

$$\lambda \geq 0, \quad \phi(\boldsymbol{\tau}, q) \leq 0 \text{ and } \lambda\,\phi(\boldsymbol{\tau}, q) = 0.$$

Here $\boldsymbol{\tau} := \boldsymbol{P}\boldsymbol{F}^{-T}$ is the Kirchhoff stress tensor and $\overset{\triangledown}{\boldsymbol{\tau}} := \dot{\boldsymbol{\tau}} - \boldsymbol{w}\boldsymbol{\tau} + \boldsymbol{\tau}\boldsymbol{w}$ its Jaumann derivative, $\phi(\boldsymbol{\tau}, q) := \hat{\phi}(\boldsymbol{\tau}) + q - \sigma_Y$ is the yield criterion and $\sigma_Y > 0$ is the flow stress. We assume that $\hat{\phi}(\cdot)$ is convex function, homogeneous of degree one. In addition, the spatial elasticity tensor $\mathbf{c}$ is assumed to possesses the usual symmetry conditions and remains positive definite, in the sense that $\boldsymbol{\tau} \cdot \mathbf{c}^{-1}\boldsymbol{\tau} \geq \beta_0\|\boldsymbol{\tau}\|^2$ with $\beta_0 > 0$ and arbitrary $\boldsymbol{\tau} = \boldsymbol{\tau}^T$. To illustrate the key results, it suffices to consider the simplest model of *softening plasticity* in which

$$\alpha = -\mathcal{H}^{-1}q \quad \text{with} \quad \mathcal{H} = \text{constant} < 0. \tag{3.13}$$

The case $\mathcal{H} > 0$ corresponds to hardening plasticity. Observe that the flow rule $(3.12)_2$ implies that the plastic spin $\boldsymbol{w}^p \equiv \boldsymbol{0}$ since $\partial_{\boldsymbol{\tau}}\phi$ is symmetric.

REMARK 3.3. The preceding model can be shown to arise as the rate form of multiplicative multiplicative plasticity, with

$$\boldsymbol{l}^e = \dot{\boldsymbol{F}}^e\boldsymbol{F}^{e-1} \quad \text{and} \quad \boldsymbol{l}^p := \boldsymbol{F}^e\boldsymbol{L}^p\boldsymbol{F}^{e-1}, \quad \text{where} \quad \boldsymbol{L}^p = \dot{\boldsymbol{F}}^p\boldsymbol{F}^{p-1}. \tag{3.14}$$

The Kirchhoff stress tensor is defined in terms of a stored energy function $W(C^e)$ via the hyperelastic constitutive equation

$$\boldsymbol{\tau} = \boldsymbol{F}^e\left[2\partial_{\bar{C}^e}W(C^e)\right]\boldsymbol{F}^{eT} \quad \text{where} \quad C^e = \boldsymbol{F}^{eT}\boldsymbol{F}^e. \tag{3.15}$$

The spatial elastic moduli $\mathbf{c}$ are given by the standard relation

$$\mathbf{c}_{ijkl} = F^e_{iI}F^e_{jJ}F^e_{kK}F^e_{lL}\frac{\partial^2 W}{\partial C^e_{IJ}\partial C^e_{KL}}. \tag{3.16}$$

Finally, the local plastic dissipation $\mathcal{D}$ predicted by model, defined as he local stress power minus the rate of change of the internal energy, equals the flow stress times the plastic slip, i.e.,

$$\mathcal{D} = \lambda\tau_Y \geq 0, \quad \text{since } \lambda \geq 0. \tag{3.17}$$

A detailed proof of the preceding results is given in Simo [1994].   ■

The goal of the analysis below is to identify the conditions that render the constitutive model (3.12) with the softening law (3.13) mathematically consistent with expression (3.7a) for the spatial velocity gradient l, which involves a *delta*–measure. We proceed in two steps.

i. First, by inserting (3.7a,b) into into the rate constitutive equations (3.12) one arrives at the following expression

$$\mathbf{c}^{-1}\overset{\triangledown}{\tau} - \bar{l} = \delta_\mathcal{S}\text{sym}\left[L_{\bar{\boldsymbol{v}}}[\![\varphi]\!] \otimes \boldsymbol{n}\right] - \lambda\partial_\tau\phi. \tag{3.18}$$

Now, the left-hand-side of this equation is a piecewise smooth function since $\bar{l}$ is piecewise smooth and the stress field τ can experience at most jump discontinuities (i.e., τ is of bounded oscillation). The right-hand-side of this equation, on the other hand, exhibits a term involving a δ–measure. Since both factor multiplying $\delta_\mathcal{S}$ is a smooth function defined on $\mathcal{S}$ and the term $\partial_\tau\phi$ are piecewise smooth, equation (3.18) can make sense mathematically only if the plastic multiplier λ itself is a distribution of the form

$$\lambda = \bar{\bar{\lambda}} + \bar{\lambda}\delta_\mathcal{S} \quad \text{where} \quad \bar{\lambda} : \mathcal{S} \to \mathbb{R} \tag{3.19}$$

is smooth and non–negative and corresponds to localized plastic deformation on the surface $\mathcal{S}$. The function $\bar{\bar{\lambda}} : \Omega \to \mathbb{R}$ is a piecewise smooth and non–negative and corresponds to diffuse yielding in the solid. Relations (3.18) and (3.19) then imply that

$$\text{sym}\left[L_{\bar{\boldsymbol{v}}}[\![\varphi]\!] \otimes \boldsymbol{n}\right] = \bar{\lambda}\partial_\tau\phi \quad \text{on} \ \mathcal{S} \times \mathsf{I}, \tag{3.20}$$

We shall refer to this result as the localization condition. Without loss of generality, in what follows it will be assumed that $\bar{\bar{\lambda}} \equiv 0$ (localized plastic deformation) so that (3.18) reduces to

$$\overset{\triangledown}{\tau} = \mathbf{c}\bar{l} \quad \text{in} \ \Omega\backslash\mathcal{S} \times \mathsf{I} \quad \text{and} \quad \lambda = \bar{\lambda}\delta_\mathcal{S}. \tag{3.21}$$

In other words, the region $\Omega\backslash\mathcal{S}$ remains elastic, in agreement with the simplifying assumption that $\bar{\bar{\lambda}} \equiv 0$.

ii. By inserting the softening law (3.13) into the evolution equation (3.12)$_3$ for the softening parameter α, noting that $\partial_q\phi = 1$ and using expression (3.19), one obtains

$$H^{-1}\dot{q} = -\dot{\alpha} = -\bar{\lambda}\delta_\mathcal{S}. \tag{3.22}$$

Now, the stress–like hardening variable q must remain a piecewise smooth function if the yield criterion $\phi(\tau, q) \leq 0$ is to retain its classical interpretation. It follows that the

preceding relation can remain mathematically meaningful only if the softening modulus itself is a distribution, i.e.,

$$\mathcal{H}^{-1} = \bar{\mathcal{H}}^{-1}\,\delta_\mathcal{S} \quad \text{where} \quad \bar{\mathcal{H}} = \text{constant} < 0. \tag{3.23}$$

This result is amenable to a compelling physical interpretation which relates $\bar{\mathcal{H}}$ to the fracture energy of the material, see Simo, Oliver & Armero [1993]. A similar interpretation holds for damage models (Oliver & Simo [1994]).

The localization condition (3.20) can be cast into the following equivalent form

LEMMA 3.2. Let $Q_\mathcal{S}^{ep}$ denote the perfectly plastic spatial acoustic tensor evaluated on the surface $\mathcal{S}$ via the conventional expression

$$Q_\mathcal{S}^{ep} := n \left[\mathbf{c} - \frac{\mathbf{c}\partial_\tau\phi \otimes \mathbf{c}\partial_\tau\phi}{\partial_\tau\phi : \mathbf{c}\partial_\tau\phi} \right]_\mathcal{S} n \quad (\text{for } \lambda > 0). \tag{3.24}$$

Then the localization condition (3.20) is equivalent to the requirement

$$Q_\mathcal{S}^{ep} L_{\bar{v}}[\varphi] = 0 \iff \text{Ker}[Q_\mathcal{S}^{ep}] \neq \emptyset. \tag{3.25}$$

which holds in and only if the condition $\det[Q_\mathcal{S}^{ep}] = 0$ holds.

PROOF. Multiplying both sides of (3.20) by $\mathbf{c}\partial_\tau\phi$ and contracting the result with $\partial_\tau\phi$ yields the following expression for the multiplier: $\bar{\lambda}$

$$\bar{\lambda} = \frac{1}{\partial_\tau\phi : \mathbf{c}\partial_\tau\phi}\,\partial_\tau\phi : \mathbf{c}\,[L_{\bar{v}}[\varphi] \otimes n]. \tag{3.26}$$

By applying the tensor $\mathbf{c}$ to both sides of the localization condition (3.20) and the result to the normal n one obtains

$$[\,n\,\mathbf{c}\,n\,] L_{\bar{v}}[\varphi] - \bar{\lambda}\,[\,\mathbf{c}\,\partial_\tau\phi\,]\,n = 0 \tag{3.27}$$

Inserting (3.26) into (3.27) and rearranging terms yields (3.25) and hence the result. ∎

It is worth pointing out that the localization condition (3.25) in terms of the acoustic tensor does not involve the softening parameter $\bar{\mathcal{H}}$. This is in sharp contrast with similar conditions derived in the literature by means of the Thomas-Hill-Mandel analysis of weak discontinuities (acceleration waves), see e.g. Needleman & Tvergard [1992]. An identical condition holds, therefore, for the perfectly plastic case corresponding to $\bar{\mathcal{H}} = 0$.

3.3 The Limiting Problem: Plastic Flow on the Slip Surface $\mathcal{S}$

By virtue of Assumption 3.1, $\bar{\varphi}(\mathcal{S})$ is a slip surface since $[\![\varphi]\!] \cdot \boldsymbol{n} = 0$. Our goal below is to identify the reduced problem that governs plastic flow on the slip surface $\mathcal{S}$. To do so observe first that $\mathcal{S}$ is a material surface and, therefore, $\dot{\boldsymbol{N}} = 0$. As a result, since $\boldsymbol{n} = \bar{F}^{-T}\boldsymbol{N}$, it follows that $L_{\bar{v}}\boldsymbol{n} = 0$. Time differentiation of the slip condition then yields the additional relation

$$0 = \frac{d}{dt}\left([\![\varphi]\!] \cdot \boldsymbol{n}\right) = L_{\bar{v}}[\![\varphi]\!] \cdot \boldsymbol{n} + [\![\varphi]\!] \cdot L_{\bar{v}}\boldsymbol{n} \implies L_{\bar{v}}[\![\varphi]\!] \cdot \boldsymbol{n} = 0. \tag{3.28a}$$

Now let $\{\boldsymbol{t}_1, \boldsymbol{t}_2, \boldsymbol{n}\}$ denote the convected basis at $\boldsymbol{y} = \bar{\varphi}(\mathcal{S})$, so that $\boldsymbol{t}_\alpha = \bar{F}\boldsymbol{Y}_{,\alpha}$ is a normal parametrization of $\mathcal{S}$. Since $\bar{\varphi}(\mathcal{S})$ is convected by the flow of $\bar{v}$ it follows that

$$\boldsymbol{t}_\alpha \cdot \boldsymbol{n} = 0 \quad \text{for} \quad \alpha = 1, 2. \tag{3.28b}$$

The localization condition (3.20) together with (3.28a,b) then yield the following results.

i. By contracting both sides of (3.20) with $\boldsymbol{n} \otimes \boldsymbol{n}$ and $\boldsymbol{t}_\alpha \otimes \boldsymbol{t}_\beta$, $\alpha, \beta = 1, 2$ one obtains

$$\boldsymbol{n} \cdot [\partial_\tau \phi]\boldsymbol{n} = 0 \quad \text{and} \quad \boldsymbol{t}_\alpha \cdot [\partial_\tau \phi]\boldsymbol{t}_\beta = 0 \quad \text{for} \quad \alpha, \beta = 1, 2, \tag{3.29a}$$

while, in general,

$$\tau_\alpha := \boldsymbol{t}_\alpha \cdot [\partial_\tau \phi]\boldsymbol{n} \neq 0 \quad \text{for} \quad \alpha = 1, 2. \tag{3.29b}$$

Observe that for J_2–flow theory $\partial_\tau \phi = \text{dev}[\tau]$, where $\text{dev}[\tau]$ stands for the (Kirchhoff) stress deviator. Therefore, for J_2–flow theory conditions (3.29a,b) assert that the only non-zero stresses on a slip–surface are the *resolved shears* τ_α. Motivated by this interpretation, in the general case we shall refer to τ_α defined by (3.29b) as the *generalized resolved shears*.

ii. Since $\mathcal{S}$ is material and $\boldsymbol{t}_\alpha$ are convected by $\bar{\varphi}(\mathcal{S})$, it follows that

$$\frac{d}{dt}\left([\![\varphi]\!] \cdot \boldsymbol{t}_\alpha\right) = L_{\bar{v}}[\![\varphi]\!] \cdot \boldsymbol{t}_\alpha \quad \text{since} \quad L_{\bar{v}}\boldsymbol{t}_\alpha = 0. \tag{3.30}$$

Therefore, by contracting both sides of (3.20) with $\boldsymbol{n} \otimes \boldsymbol{t}_\alpha$, $\alpha = 1, 2$ and using results (3.28a,b) together with (3.30) one obtains

$$\frac{d}{dt}\left([\![\varphi]\!] \cdot \boldsymbol{t}_\alpha\right) = L_{\bar{v}}[\![\varphi]\!] \cdot \boldsymbol{t}_\alpha = 2\lambda\tau_\alpha, \quad \alpha = 1, 2. \tag{3.31}$$

It is clear that $\xi_\alpha = [\![\varphi]\!] \cdot \boldsymbol{t}_\alpha$ represent the components of the plastic slip taking place on the surface $\mathcal{S}$. Moreover, since $\hat{\phi}(\tau)$ is homogeneous of degree one, the yield criterion on $\mathcal{S}$ can be written as

$$\phi(\tau, q)|_\mathcal{S} = \phi_\mathcal{S}(\tau_\alpha, \alpha) := \sqrt{\tau_1^2 + \tau_2^2} - [\bar{\mathcal{H}}\alpha + \tau_Y] \leq 0. \tag{3.32}$$

As a result, the evolution equations $(3.12)_{2,3,4}$ collapse to the following problem posed on the slip surface $\mathcal{S}$:

$$\left.\begin{aligned} \dot{\xi}_\alpha &= 2\lambda\,\tau_\alpha \\ \dot{\alpha} &= \lambda \end{aligned}\right\} \tag{3.33}$$

$$\lambda \geq 0, \quad \phi_\mathcal{S}(\tau_\alpha, \alpha) \leq 0 \text{ and } \lambda\,\phi_\mathcal{S}(\tau_\alpha, \alpha) = 0.$$

It is interesting to observe that this problem is the mathematical transcription of the classical Schmidt law, which asserts that plastic flow on a slip surface is proportional to the resolved shear stress for J_2–flow theory. See Asaro [1983] for a micromechanical motivation of Schmidt law.

REMARK 3.4. The numerical implementation of the distributional character of the hardening law can be achieved in two alternative ways. First one can work directly with the standard problem (3.12) or, equivalently, with the model of multiplicative plasticity described Remark 3.3. Effective numerical algorithms for the latter form of the model are described in Simo [1992]. The distributional character of the softening law is incorporated into the algorithm by replacing the delta function $\delta_\mathcal{S}$ in the softening law (3.13) with a delta-sequence, as described in the next section. Alternatively, one can work directly with the limiting problem (3.33) thus by-passing the use of δ–sequences. Both approaches yield excellent results which are totally mesh independent. The former approach, however, has the advantage of involving only a trivial modification of existing algorithms. ∎

4 A New Finite Element Method for Localization

The boundary value problem to be solved numerically consists of the weak form (2.11) of the equilibrium equations, with test functions lying in the space $\mathcal{V}$ defined by (2.12), supplemented by the constitutive model described above. A key condition to be satisfied by the spatial discretization emanates from the analysis and conclusions summarized in the preceding section, if the features exhibited by the continuum solution are to be accurately reproduced by the numerics. The discretization must be able to replicate strain fields that exhibit bounded measures (i.e., delta functions) in order to capture both the localized plastic deformation and the distributional character of the softening law that render mesh-insensitive numerical solutions. It is well–known that he standard Galerkin finite element method cannot meet such a condition, thus leading to overly diffused results that exhibit a strong mesh dependence. The technique described below falls within the class of Assumed Enhanced Strain (AES) methods proposed in Simo & Rifai [1990] and subsequenty generalized to the finite deformation regime in Simo & Armero [1992] and Simo, Armero & Taylor [1993]. Within this framework, the preceding requirement is achieved via a particular local enrichment of the deformation field.
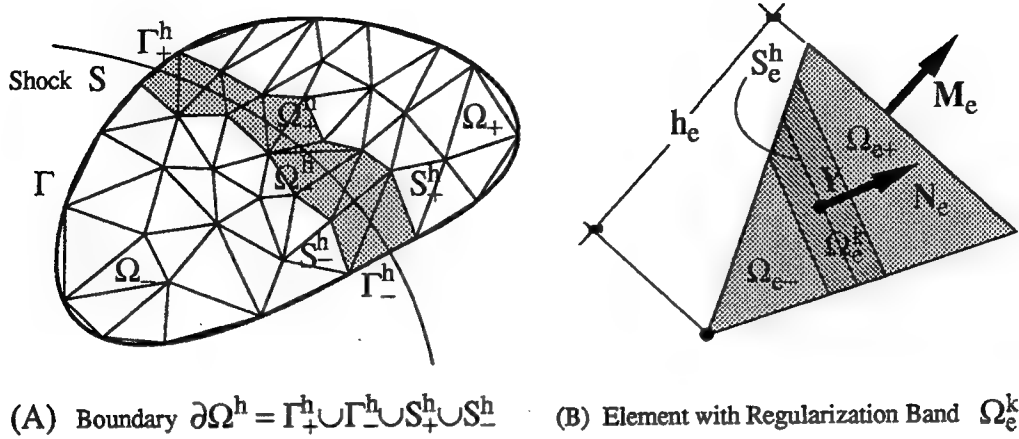
(A) Boundary $\partial\Omega^h = \Gamma^h_+\cup\Gamma^h_-\cup S^h_+\cup S^h_-$ (B) Element with Regularization Band Ω^k_e

FIGURE 4.1. (A) Finite Element discretization. Definition of the subdomain Ω^h with boundary $\partial\Omega^h$. (B) A typical element, with constant normal N_e to the element shock S^h_e and local domain Ω^k_e involved in the construction delta-sequences.

4.1 A Class of Assumed Enhanced Strain Methods

Consider a standard finite element discretization $\Omega \approx \cup^E_{e=1}\Omega_e$ of the domain Ω with characteristic mesh–size $h > 0$, as shown in Figure 4.1. We introduce at the outset the decomposition (2.6) of the displacement field, with associated test functions lying in the space $\mathcal{V}$ defined by (2.12). For convenience, we shall denote by $\bar{\mathcal{V}}$ the space spanned by the regular part $\bar{\eta}$ of the test functions $\eta = \bar{\eta} + M_S\beta \in \mathcal{V}$.

The key idea in the method described below is to work directly in terms of the *regular* part of the displacement field and the admissible test functions, which are amenable to a conventional C^0-finite element approximation $\bar{\mathcal{V}}^h \subset \bar{\mathcal{V}}$. For the sake of concreteness, consider an approximation via constant strain triangles of tetrahedra, i.e,

$$\bar{\mathcal{V}}^h := \left\{\bar{\eta}^h \in [C^0(\Omega)]^{n_{\dim}} : \bar{\eta}^h_e \in [P^1(\Omega_e)]^{n_{\dim}} \quad \text{and} \quad \bar{\eta}^h\Big|_{\Gamma_t} = 0\right\}. \qquad (4.1)$$

The singular (distributional) character of the strain field in the continuum problem is captured within the proposed numerical approach via a *local* enhancement at the element level; i.e., by considering enhanced deformation gradients F^h with associated variations denoted by G^h of the form

$$F^h_e = \underbrace{\text{GRAD}[\bar{\varphi}^h]}_{\text{Galerkin}} + \underbrace{\tilde{F}^h_e}_{\text{Enhanced}} \quad \text{and} \quad G^h_e = \underbrace{\text{GRAD}[\bar{\eta}^h]}_{\text{Galerkin}} + \underbrace{\tilde{G}^h_e}_{\text{Enhanced}} . \qquad (4.2)$$

We denote by $\tilde{\mathcal{E}}^h_\epsilon$ the finite element spaces of enhanced strains $\tilde{F}^h$ and let $\tilde{\mathcal{E}}^h_\gamma$ be the corresponding weighting space of admissible variations. In general we may have $\tilde{\mathcal{E}}^h_\epsilon \neq \bar{\mathcal{E}}^h_\gamma$, a situation reminiscent of the so–called Petrov–Galerkin formulations. A key additional

condition placed on both $\tilde{\mathcal{E}}_\varepsilon^h$ and $\tilde{\mathcal{E}}_\gamma^h$ is that the finite element approximations be *discontinuous between elements*. Within this context, the appropriate variational formulation of the discretized finite element problem is given by the following system:

$$\left.\begin{aligned}\int_\Omega \boldsymbol{P}^h : \text{GRAD}[\bar{\boldsymbol{\eta}}^h]\, d\Omega = \int_\Omega \boldsymbol{f} \cdot \bar{\boldsymbol{\eta}}^h\, d\Omega + \int_{\Gamma_t} \boldsymbol{t} \cdot \bar{\boldsymbol{\eta}}^h\, d\Gamma, \quad \forall \bar{\boldsymbol{\eta}}^h \in \bar{\mathcal{V}}^h, \\ \int_{\Omega_e} \boldsymbol{P}^h : \tilde{\boldsymbol{G}}_e^h\, d\Omega = 0, \quad \forall \tilde{\boldsymbol{G}}^h \in \tilde{\mathcal{E}}_\gamma^h \quad \text{and} \quad e = 1, 2, \cdots, E.\end{aligned}\right\} \quad (4.3)$$

The nominal stress field $\boldsymbol{P}^h$ in (4.3) is computed via the specific constitutive model under consideration, but evaluated with the *enhanced strain field* defined by $(4.2)_1$. The design of the weighting space $\tilde{\mathcal{E}}_\gamma^h$ is restricted by the following key conditions set forth in Simo & Armero [1992], which ensure stability and consistency of the of the AES method.

i. *Consistency*: For the linear interpolations (4.1), strains in $\tilde{\mathcal{E}}_\gamma^h$ must have zero element mean, i.e., $\int_{\Omega_e} \tilde{\boldsymbol{G}}_e^h\, d\Omega = 0$ for all $\tilde{\boldsymbol{G}}^h \in \tilde{\mathcal{E}}_\gamma^h$.

ii. *Stability*: The space $\text{GRAD}[\bar{\mathcal{V}}^h]$ of strains associated with test functions in $\bar{\mathcal{V}}^h$ and the space $\tilde{\mathcal{E}}_\gamma^h$ must have null intersection; i.e, $\text{GRAD}[\bar{\mathcal{V}}^h] \cap \tilde{\mathcal{E}}_\gamma^h = \varnothing$.

For a convergence proof restricted to linear problems see Reddy & Simo [1992].

4.2 Design of the Enhanced Strain Fields

To describe the proposed construction, it is convenient to suppose for the moment that the material surface $\mathcal{S}$ is given. Furthermore, for simplicity we restrict our subsequent developments to the case $n_{\text{dim}} = 2$. The case $n_{\text{dim}} = 1$ is described in detail in Simo, Oliver & Armero [1993]. Consistent with the linear interpolation in (4.1), we assume that the approximation $\mathcal{S}^h$ to $\mathcal{S}$ is a polygonal line, with vertices lying on the sides of the triangular elements, which intersect an element Ω_e along the segment $\mathcal{S}_e^h$ with constant unit normal $\boldsymbol{N}_e$. Let J denote the set of numbers associated with elements that intersect $\mathcal{S}^h$, i.e.,

$$J := \left\{ e \in \{1, 2, ..., E\} : \Omega_e \cap \mathcal{S}^h \neq \varnothing \right\}. \quad (4.4)$$

Now let N be the global node numbers associated with the elements Ω_e intersecting $\mathcal{S}^h$; i.e., such that $e \in J$. We set $N = N_+ \cup N_-$, where N_+ (respectively N_-) are the global node numbers in N associated with nodes lying ahead of (behind of) the shock $\mathcal{S}^h$. Clearly, the polygonal lines with nodal points associated with the sets $N^\pm$ define approximations (also denoted by $\mathcal{S}_\pm^h$) to the lines $\mathcal{S}_\pm^h$ introduced in Section 2, see Figure 2. With this notation at hand we proceed as follows.

(A) *Construction of the space* $\tilde{\mathcal{E}}_\varepsilon^h$. Assuming that the jump $[\![\varphi]\!]$ in the motion is constant within a typical element Ω_e, $e \in J$, and in view of the decomposition (2.6) for
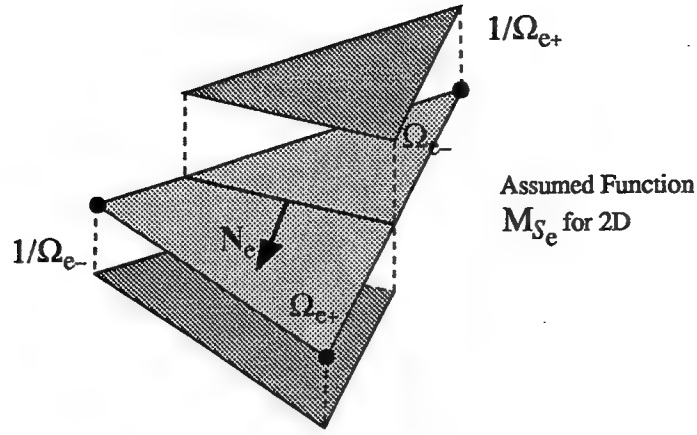
FIGURE 4.2. Restriction of the function M_S to a typical element Ω_e

the displacement field, it is natural to adopt the following approximation for the enhanced strain field:

$$\tilde{\mathcal{E}}_\varepsilon^h := \left\{ \tilde{F}^h \in [L^2(\Omega)]^2 \times [L^2(\Omega)]^2 : \tilde{F}_e^h = \alpha_e \otimes \text{GRAD}[M_{S_e}^h] \text{ with } \alpha_e \in \mathbb{R}^2 \right\}. \quad (4.5)$$

Here α_e are element parameters, which are suppose to replicate the jump within the element. In addition, $M_{S_e}^h$ is the restriction to the element Ω_e of an approximation to the function M_S that satisfies the two conditions **i** and **ii** set forth in Section 2.2 and is constructed as follows.

For a typical element Ω_e with $e \in J$, $\mathcal{S}^h$ intersect two sides of Ω_e with common node which will be denoted in what follows by X_e^*. Let N_e^* denote the element shape function associated with this node. Denoting by $h_e > 0$ the distance from X_e^* to the opposite side, with unit outward normal M_e (see Figure 4.1), we have

$$N_e^*(X) := 1 - (X - X_e^*) \cdot M_e \Big/ h^e \quad \text{with} \quad |M_e| = 1. \quad (4.6)$$

The function M_S^h is then obtained as the assembly of local element functions M_{S_e} defined as (see Figure 4.1)

$$M_{S_e} := \bar{H}_{S_e} - N_e^* \quad \text{where} \quad \bar{H}_{S_e}(X) := \begin{cases} 1 & \text{if } X \in \Omega_{e-}, \\ 0 & \text{if } X \in \Omega_{e+}. \end{cases} \quad (4.7)$$

Here Ω_{e+} and Ω_{e-} are the regions within the element ahead and behind of the shock. This definition clearly ensures that $[\![M_S]\!] = 1$ (condition **i**) while vanishing outside of the region region Ω^h limited by the polygonals $\mathcal{S}_\pm^h$ and the boundary of the body (condition **ii**). The gradient of the function M_{S_e} is given by the expression

$$\text{GRAD}[M_{S_e}] := \delta_{S_e} N_e - \frac{1}{h_e} M_e, \quad (4.8)$$
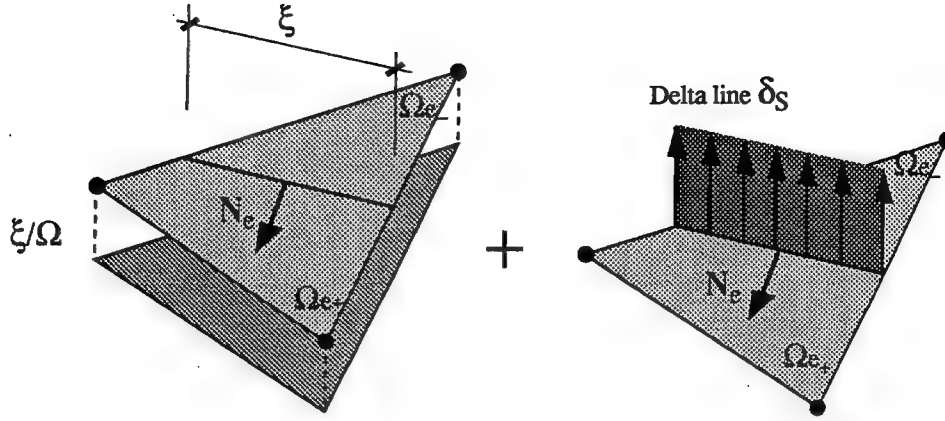
FIGURE 4.3. Illustration of the gradient GRAD[M_S] for a typical element Ω_e

which is illustrated in Figure 4.3.

REMARK 4.1. In the actual implementation of (4.7) the H-function $\bar{H}_{S_e}$ is replaced by an H–sequence. Such a sequence is constructed by replacing the straight segment $\mathcal{S}_e^h$ with a narrow band of thickness k denoted by Ω_e^k. The derivative of the function M_{S_e} regularized in such a way, which is denoted by $M_{S_e}^k$, is given by (see Figure 4.4)

$$\text{GRAD}[M_{S_e}^k] := \delta_{S_e}^k N_e - \frac{1}{k} M_e \quad \text{where} \quad \delta_{S_e}^k = \begin{cases} 1/k & \text{if } X \in \Omega_e^k, \\ 0 & \text{otherwise .} \end{cases} \tag{4.9}$$

Observe that $M_e = N_e$ *only if* the shock $\mathcal{S}_e^h$ is aligned with the mesh. The regularization parameter $k > 0$ is unrelated to the characteristic mesh size parameter h and is chosen as small as possible *for fixed, finite h*, within the limitations imposed by machine precision. Within this context, enforcement of the distributional character of the hardening law becomes trivial: The delta-sequence (4.9)$_2$ induces the corresponding delta-sequence for the (inverse of the) softening modulus

$$\mathcal{H}_S^k(X) = \begin{cases} k\bar{\mathcal{H}} & \text{if } X \in \Omega_e^k, \\ \infty & \text{otherwise .} \end{cases} \tag{4.10}$$

The value $\mathcal{H}_S^k(X) = \infty$ for $X \notin \Omega_e^k$ is consistent with elastic behavior outside the localization band. This approach is totally unrelated to the so-called characteristic length, an ad-hoc concept widely used in smeared crack models, see e.g., Hilerborg [1985], Bazant [1986] and Oliver [1989] for the best available version. ∎

The proposed assumed enhanced strain approach is clearly strain driven and fits, therefore, the usual framework of constitutive integration algorithms (see Simo [1992] for a comprehensive review). In particular, for the models described in the preceding Section,
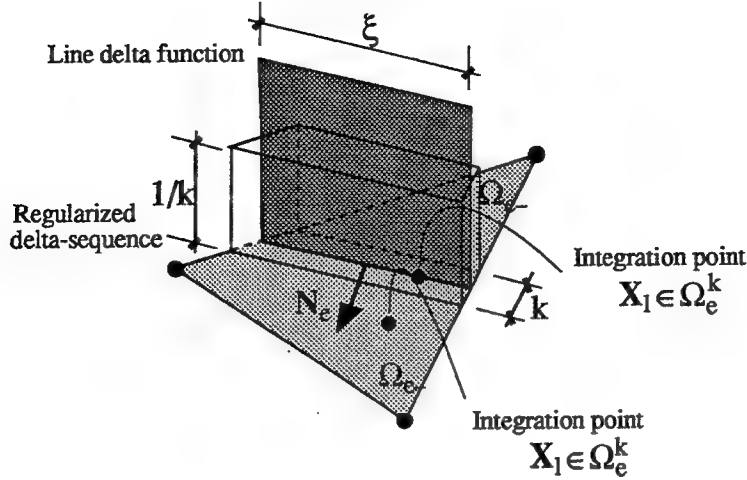
FIGURE 4.4. Illustration of the regularized gradient $\mathrm{GRAD}[M_{\mathcal{S}_e}^k]$ within a typical element Ω_e.

the standard return mapping algorithms remain unchanged; the only modification needed is the replacement of the softening modulus with the sequence (4.10).

(B) *Construction of the weighting space* $\tilde{\mathcal{E}}_\gamma^h$. The choice adopted below is motivated by the proof of part (ii) in Lemma 2.1, where condition $(2.13b)_2$ is obtained essentially by considering in the weak form (2.11) the continuum counterpart of the enhanced variations $\tilde{G}^h$ appearing in $(4.2)_2$. Relative to a normal parametrization $\boldsymbol{X}_e = \boldsymbol{Y}_e + \eta \boldsymbol{N}_e$, where $\boldsymbol{Y}_e$ is on the segment $\mathcal{S}_e^h$ and $-k \leq \eta \leq k$, we set

$$\tilde{\mathcal{E}}_\gamma^h := \left\{ \tilde{G}^h \in [L^2(\Omega)]^2 \times [L^2(\Omega)]^2 : \tilde{G}_e^h = \left[\delta_{\mathcal{S}_e}^k - \psi^{k\prime} \right] (\beta_e \otimes \boldsymbol{N}_e), \ \alpha_e \in \mathbb{R}^2 \right\}. \quad (4.11)$$

The function $\psi^k(\eta)$ arbitrary although restricted by the condition $\psi^k(\eta)|_{\eta=k} - \psi^k(\eta)|_{\eta=-k} = 1$ which ensures satisfaction of the stability condition on $\tilde{\mathcal{E}}_\gamma^h$. Observe carefully that $\tilde{\mathcal{E}}_\gamma^h \neq \tilde{\mathcal{E}}_\varepsilon^h$ except in the case $\boldsymbol{M}_e = \boldsymbol{N}_e$ where the shock is aligned with one triangle side. The ultimate justification for (4.11) lies on the following result which furnishes the finite element counterpart of relation $(2.13)_2$:

$$\int_{\Omega_e} \tilde{G}_e^h : \boldsymbol{P}^h \, d\Omega = 0 \quad \forall \tilde{G}^h \in \tilde{\mathcal{E}}_\gamma^h \iff \boldsymbol{P}_+^h \boldsymbol{N}_e = \boldsymbol{P}_{\mathcal{S}_e}^h \boldsymbol{N}_e. \quad (4.12)$$

Here $\boldsymbol{P}_{\mathcal{S}_e}^h$ is the stress on the band Ω_e^k and $\boldsymbol{P}_+^h$ is the stress on the region $[\Omega_e \backslash \Omega_e^k] \cap \Omega_{e+}$ ahead of the shock. The proof of this relation is straightforward and follows from the fact that $\boldsymbol{P}^h$ is piecewise constant. Observe that the jump condition $[\![\boldsymbol{P}_e^h]\!] \boldsymbol{N}_e = 0$ is proved exactly as in Lemma 2.1. Finally, from definition (4.11) it is immediate to verify the $\tilde{\mathcal{E}}_\gamma^h \cap \mathrm{GRAD}[\bar{\mathcal{V}}^h] = \emptyset$. Hence, $\tilde{\mathcal{E}}_\gamma^h$ defined by (4.11) satisfies the consistency and the stability requirements for AES methods.

4.3. A Representative Numerical Simulation.

To illustrate the preceding methodology we consider the isotropic damage model described in Oliver & Simo [1994] in an uni-axial tension test. It can be shown (see the preceding reference) that the localization condition determines the angle ϑ between the normal N and the loading direction e as $\vartheta = \sqrt{\nu}$, where ν is the Poisson's ratio. A typical numerical result for $\nu = 0.4$ is shown in Figure 4.5 for a completely *non-structured* finite element mesh. The computed deformed shape of the specimen, shown in Figure 4.5, shows that the entire deformation takes place in the band of elements intersecting a straight line at $\pi/2 + \vartheta$, as expected. Outside the band the deformation is elastic and, therefore, the specimen behaves nearly as two rigid solids sliding with respect to each other. The load displacement curve, not shown in the figure, exhibits absolutely no mesh dependence.
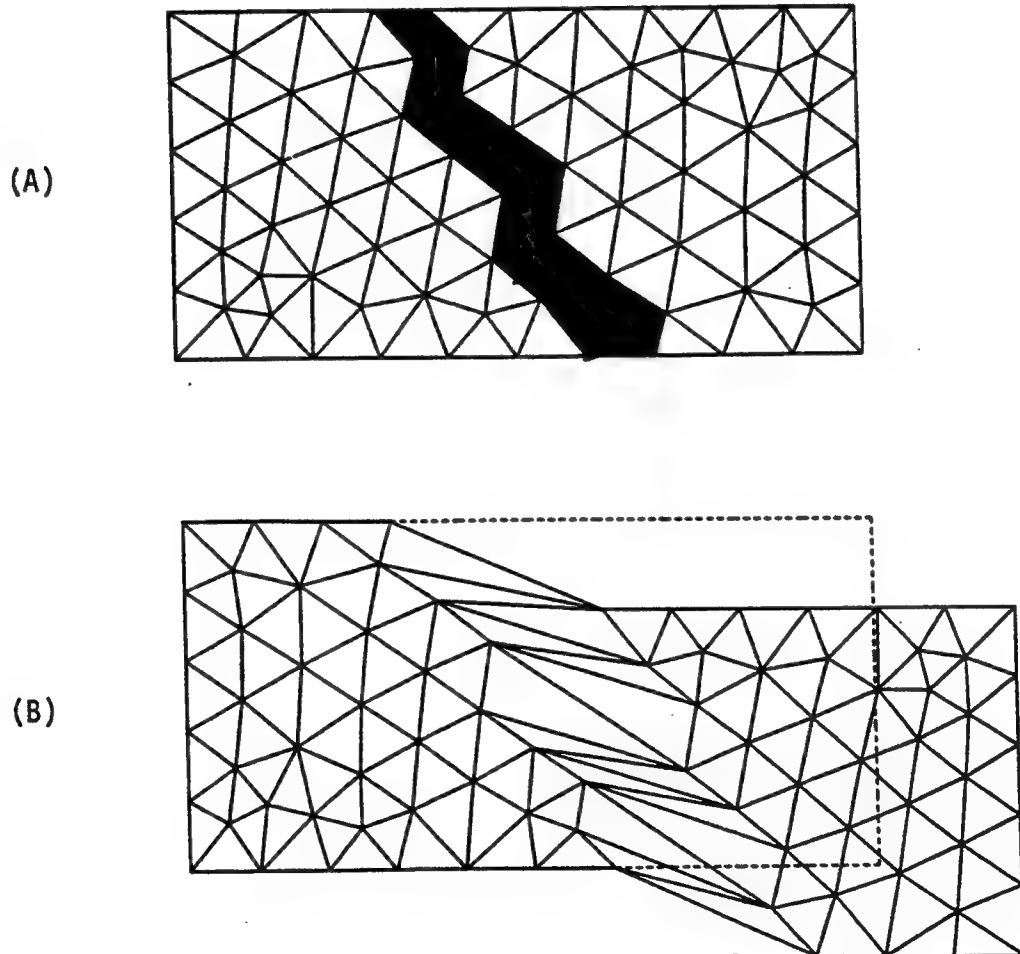
(A)

(B)

FIGURE 4.5. Uniaxial tension test for an isotropic damage model. (A) Non-structured finite element mesh and computed domain Ω^h containing the shock S^h. (B) Computed deformed shape exhibiting the strong localization.

References

[1] Asaro, R. [1983] "Micromechanics of crystals and polycrystals", in *Advances in Applied Mechanics*, ed. by T.Y. Wu, J.W. Hutchinson, **23**, 1-115.

[2] Z.P. Bazant [1986] "Mechanics of Distributed Cracking", *Applied Mechanics Review*, **5**, 675-705.

[3] S. Govindjee, G.J. Kay and J.C. Simo [1994] "Anisotropic Modeling and Numerical Simulation of Brittle Damaga in Concrete," submitted to *International Journal for Numerical Methods in Engineering.*

[4] A. Hillerborg [1985] "Numerical Methods to Simulate Softening and Fracture of Concrete," in *Fracture Mechanics of Concrete: Structural Application and Numerical Calculation*, ed. by G.C. Sih and A. DiTommaso, 141-170.

[5] R. Larson, K. Runesson and N.S. Otosen [1994] "Discontinuous Displacement Approximation for Capturing Plastic Localization," *International Journal for Numerical Methods in Engineering*, **36**, 2087-2105.

[6] E.H. Lee [1969] "Elastic-Plastic Deformations at Finite Strains", *Journal of Applied Mechanics*, **36**, 1-6.

[7] E. Mamiya and J.C. Simo [1994] "Numerical Simulation of Equilibrium Shocks in Maximally Dissipative Systems", *Journal of Elasticity,* in press.

[8] J. Mandel [1974] "Thermodynamics and Plasticity", in *Foundations of Continuum Thermodynamics,* ed. by J.J. Delgado Dominguez, N.R. Nina and J.H. Whitelaw, 283-304.

[9] A. Needleman and V. Tvergaard [1992] "Analysis of Plastic Localization in Metals", *Applied Mechancis Reviews*, 3-18.

[10] J. Oliver [1989] "A Consistent Characteristic Length for Smeared Cracking Models", *International Journal for Numerical Methods in Engineering*, **28**, 461-474.

[11] J. Oliver and J.C. Simo [1994] "Modeling Strong Discontinuities by Means of Strain Softening Constitutive Equations", *EURO-C, Computational Modeling of Concrete Structures*, **28**, 461-474.

[12] D. Reddy and J.C. Simo [1992] "Stability and Convergence Analysis of a Class of Assumed Strain Mixed Methods", *SIAM Journal of Numerical Analysis*, **28**, 461-474.

[13] J.C. Simo and J.W. Ju [1984] "A Continuum Strain Based Damage Model. Part I: Formulation. Part II: Numerical Algorithms", *International Journal of Solids and Structures,* **23**, 821-840 and 841-871.

[14] J.C. Simo and M.S. Rifai [1990] "A Class of Mixed Assumed Strain Methods and the Method of Incompatible Modes", *International Journal for Numerical Methods in Engineering,* **29**, 1595-1638.

[15] J.C. Simo and F. Armero [1992] "Geometrically Nonlinear Enhanced Strain Mixed Methods and the Method of Incompatible Modes", *International Journal for Numerical Methods in Engineering,* **33**, 1413-1449.

[16] J.C. Simo [1992] "Algorithms for Multiplicative Plasticity that Preserve the Form of the Return Mappings of the Infinitesimal Theory", *Computer Methods in Applied Mechanics and Engineering,* **99**, 61-112.

[17] J.C. Simo, F. Armero and R.L. Taylor [1993] "Improved Versions of Enhanced Strain Trilinear Elements for 3D Deformation Problems", *Computer Methods in Applied Mechanics and Engineering,* **110**, 359-386.

[18] J.C. Simo and G. Meschke [1993] "A New Class of Algorithms for Classical Plasticity Extended to Finite Strains: Application to Geomaterials", *International J. Computational Mechanics,* **11**, 253-278.

[19] J.C. Simo, J. Oliver and F. Armero [1993] "An Analysis of Strong Discontinuities Induced by Softening Solutions in Rate Independent Solids", *Journal of Computational Mechanics,* **12**, 277-296.

[20] J.C. Simo. "Numerical Analysis of Classical Plasticity", in *Handbook for Numerical Analysis, Volume IV,* ed. by P.G. Ciaret and J.J. Lions, in press, 1994.

[21] J.C. Simo and J. Oliver [1994] "A New Approach to the Analysis and Simulation of Strain Softening in Solids", in *Mechanics of Distributed Cracking,* ed. by Z. Bazant, J. Marzars and A. Jirousek.

[22] C. Truesdell and R. Toupin [1960] "The Classical Field Theories", in *Handbook der Physik,* ed. by S. Flugge, 277-902.

DISTRIBUTION LIST

AC ENGRG INC / BERRY, WEST LAFAYETTE, IN
ADINA ENGRG, INC / WALCZAK, WATERTOWN, MA
AEWES / LIB, VICKSBURG, MS
AEWES / PETERS, VICKSBURG, MS
AFWL/NTE / BALADI, KIRTLAND AFB, TX
ANATECH APPLICATIONS / CASTRO, SAN DIEGO, CA
ANATECH RESEARCH CORP / RASHID, SAN DIEGO, CA
APPLIED PHYSICS TECH / SWANSON, MCLEAN, VA
APPLIED RSCH ASSOC, INC / HIGGINS, ALBUQUERQUE, NM
ARMY EWES / WES (NORMAN), VICKSBURG, MS
ARMY EWES / WESIM-C (N. RADHAKRISHNAN), VICKSBURG, MS
ASSOCIATED SCIENTISTS/ MCCOY, WOODS HOLE, MA
BING C YEN / IRVINE, CA
BRITISH EMBASSY / ELLIS, WASHINGTON, DC
BYU / ROLLINS, PROVO, UT
CALIF INST OF TECH / PASADENA, CA
CALTRANS OFFICE OF RESEARCH / HOLLAND, SACRAMENTO, CA
CATHOLIC UNIV / CE DEPT (KIM) WASHINGTON, DC
CENTRIC ENGINEERING SYSTEMS INC / TAYLOR, PALO ALTO, CA
CHALMERS UNIVERSITY OF TECHNOLOGY / TEPFERS, 412 74 GOTEBORG,
CHEUNG AND ASSOCIATES / CHEUNG, IRVINE, CA
COLORADO SCHOOL OF MINES / GOLDEN, CO
COLORADO ST UNIV / FORT COLLINS, CO
COMPUTATIONAL MECHANICS / BREBBIA SOUTHAMPTON,
CORNELL UNIV / ITHACA, NY
COUNTY OF VENTURA / TAKAHASHI, VENTURA, CA
CRREL / KOVACS, HANOVER, NH
CSU CHICO / ARTHUR, CHICO, CA
CSU FULLERTON / RAMSAMOOJ, FULLERTON, CA
DAMES & MOORE / LOS ANGELES, CA
DET NORSKE VERITAS RESEARCH AS / BERGAN, VERITASVEIEN 1, N-1322 HOVIK
DTIC / ALEXANDRIA, VA
ENVIROPLEX / AUDIBERT, HOUSTON, TX
FAU / BOCA RATON, FL
FAU / REDDY, BOCA RATON, FL
GEORGE WASHINGTON UNIV / ENGRG & APP SCI SCHL (FOX), WASHINGTON, DC
GEOTECHNICAL ENGRS, INC / MURDOCK, WINCHESTER, MA
GEOTEST INSTRUMENT CORP / BABENDREIER, SILVER SPRINGS, MD
GERWICK INC / SAN FRANCISCO, CA
GIANNOTTI & ASSOCIATES OF TEXAS INC / GIANNOTTI, VENTURA, CA
HEUZE / ALAMO, CA
HKS INC / PAWTUCKET, RI
HQ AFESC / TYNDALL AFB, FL
IOWA STATE UNIV / AMES, IA
JOHN HOPKINS UNIV / COX, BALTIMORE, MD
JOHN HOPKINS UNIV / LADE, BALTIMORE, MD
KARAGOZIAN AND CASE / CRAWFORD, GLENDALE, CA
LANTNAVFACENGCOM / CODE 411, NORFOLK, VA

LAWRENCE LIVERMORE NATIONAL LAB / MAKER, LIVERMORE, CA
LAWRENCE LIVERMORE NATIONAL LAB / MCCALLEN, LIVERMORE, CA
LAWRENCE TECH UNIV / SOUTHFIELD, ME
LEHIGH UNIV / BETHLEHAM, PA
LIN OFFSHORE ENGRG / SAN FRANCISCO, CA
LOCKHEED / RSCH LAB (M. JACOBY), PALO ALTO, CA
LOCKHEED / RSCH LAB (P UNDERWOOD), PALO ALTO, CA
MAINE MARITIME ACADEMY / LIB, CASTINE, ME
MARC ANALYSIS RSCH CORP / HSU, PALO ALTO, CA
MCCLELLAND ENGRS / HOUSTON, TX
MICHIGAN UNIV / HOUGHTON, MI
MIT / R.V. WHITMAN, CAMBRIDGE, MA
MOBILE R&D CORP / DALLAS, TX
MONTANA STATE UNIV / PERKINS, BOZEMAN, MT
NATL ACADEMY OF SCIENCES / NRC, DR. CHUNG, WASHINGTON, DC
NAVFACENGCOM / CODE 04A3, ALEXANDRIA, VA
NAVFACENGCOM / CODE 1002B, ALEXANDRIA, VA
NAVFACENGCOM / CODE 163, ALEXANDRIA, VA
NAVSHIP / CODE 245L, FPO AP,
NCSC / PANAMA CITY, FL
NEW ENGLAND MARINE RESEARCH LAB / LIB, DUXBURY, MA
NFESC ECDET / ESC61 (WU), WASHINGTON, DC
NFESC ECDET / ESC61 CECILIO, WASHINGTON, DC
NORDA / BENNETT, NSTL, MS
NORTH CAROLINA STATE UNIV / RAHMAN, RALEIGH, NC
NORTHROP / CHEN, HAWTHORNE, CA
NORTHWESTERN UNIV / LIU, EVANSTON, IL
NORTHWESTERN UNIVERSITY / EVANSTON, IL
NORTHWESTERN UNIVERSITY / BAZANT, EVANSTON, IL
NORTHWESTERN UNIVERSITY / CE DEPT (BELYTSCHKO), EVANSTON, IL
NRL / VALENT, STENNIS SPACE CENTER, MS
NSF / ASTILL, ARLINGTON, VA
NSF / STRUC & BLDG SYSTEMS (KP CHONG), WASHINGTON, DC
NTH / LANGSETH, N-7034 TRONDHEIM,
NTH / MALO, N-7034 TRONDHEIM,
NUSC / LIB, NEW LONDON, CT
NY MARITIME COLLEGE / BRONX, NY
OCNR / CODE 10P4 (KOSTOFF), ARLINGTON, VA
OCNR / CODE 1121 SILVA, ARLINGTON, VA
ONR / CODE 1132SM, ARLINGTON, VA
ONR / RAMBERG, ARLINGTON, VA
OREGON STATE UNIV / CORVALLIS, OR
OREGON STATE UNIV / CORVALLIS, OR
OREGON STATE UNIV / CE DEPT (YIM), CORVALLIS, OR
OREGON STATE UNIV / DEPT OF MECH ENGRG (SMITH), CORVALLIS, OR
PENN STATE UNIV / LAB, STATE COLLEGE, PA
PMB ENGRG / LUNDBERG, SAN FRANCISCO, CA
PORTLAND STATE UNIV / MIGLIORI, PORTLAND, OR
PURDUE UNIVERSITY / WEST LAFAYETTE, IN
SAN DIEGO STATE UNIV / SAN DIEGO, CA
SCHWER ENGR & CONSULTING SERVICES / SCHWER, BURR RIDGE, IL
SCOPUS TECHNOLOGY INC / (B NOUR-OMID), EMERYVILLE, CA
SCOPUS TECHNOLOGY INC / (S. NOUR-OMID), EMERYVILLE, CA
SEAL TEAM 6 / NORFOLK, VA

SEATTLE UNIV / SEATTLE, WA
SHANNON AND WILSON INC / SEATTLE, WA
SJSU / VUKAZICH, SAN JOSE, CA
SOUTH DAKOTA SCHOOL OF MINES AND TECH / BANG, RAPID CITY, SD
SRI INTL / ENGRG MECH DEPT (GRANT), MENLO PARK, CA
SRI INTL / ENGRG MECH DEPT (SIMONS), MENLO PARK, CA
STANFORD UNIV / APP MECH DIV (HUGHES), STANFORD, CA
STANFORD UNIV / CE DEPT (PENSKY), STANFORD, CA
STANFORD UNIV / LAW, STANFORD, CA
STATE OF CALIF / SACRAMENTO, CA
STRUCTURAL ANALYSIS PROGRAMS INC / WILSON, EL CERRITO, CA
TEXAS A&M UNIV / COLLEGE STATION, TX
TEXAS A&M UNIV / HERBICH, COLLEGE STATION, TX
TEXAS A&M UNIV / ROSCHKE, COLLEGE STATION, TX
THE EARTH TECH CORP / ARULMOLI, IRVINE, CA
TU DELFT / DE BORST, 2600 GA DELFT,
TU DELFT / VAN MIER, 2600 GA DELFT,
TUFTS UNIV / SANAYEI, MEDFORD, MA
UCLA / JU, LOS ANGELES, CA
UCSD / SCRIPPS INST OF OCEANOGRAPHY, LA JOLLA, CA
UNIV OF CAL BERKELEY / FILIPPOU, BERKELEY, CA
UNIV OF CAL BERKELEY / GOVINDJEE, BERKELEY, CA
UNIV OF CALIF BERKELEY / BERKELEY, CA
UNIV OF CALIFORNIA / MECH ENGRG DEPT (BAYO), SANTA BARBARA, CA
UNIV OF CALIFORNIA / MECH ENGRG DEPT (BRUCH), SANTA BARBARA, CA
UNIV OF CALIFORNIA / MECH ENGRG DEPT (LECKIE), SANTA BARBARA, CA
UNIV OF CALIFORNIA / MECH ENGRG DEPT (MCMEEKING), SANTA BARBARA, CA
UNIV OF CALIFORNIA / MECH ENGRG DEPT (TULIN), SANTA BARBARA, CA
UNIV OF CALIFORNIA DAVIS / CE DEPT (HERRMANN), DAVIS, CA
UNIV OF CALIFORNIA DAVIS / CE DEPT (KUTTER), DAVIS, CA
UNIV OF CALIFORNIA DAVIS / CE DEPT (RAMEY), DAVIS, CA
UNIV OF CALIFORNIA DAVIS / CTR FOR GEOTECH MODEL (IDRISS), DAVIS, CA
UNIV OF COLORADO / CE DEPT (HON-YIM KO), BOULDER, CO
UNIV OF COLORADO / MECH ENGRG DEPT (PARK), BOULDER, CO
UNIV OF CONN / LEONARD, STORRS, CT
UNIV OF CONN / LIBRARY, GROTON, CT
UNIV OF DELAWARE / NEWARK, DC
UNIV OF HAWAII / HONOLULU, HI
UNIV OF HAWAII / KANEOHE BAY, HI
UNIV OF HAWAII / HONOLULU, HI
UNIV OF HAWAII / HONOLULU, HI
UNIV OF ILLINOIS / CE LAB (PECKNOLD), URBANA, IL
UNIV OF MICH / ANN ARBOR, ME
UNIV OF N CAROLINA / CE DEPT (GUPTA), RALEIGH, NC
UNIV OF N CAROLINA / CE DEPT (TUNG), RALEIGH, NC
UNIV OF NY / BUFFALO, NY
UNIV OF RHODE ISLAND / KOVACS, KINGSTON, RI
UNIV OF RHODE ISLAND / VEYERA, KINGSTON, RI
UNIV OF TENNESSEE / KNOXVILLE, TN
UNIV OF TEXAS / JIRSA, AUSTIN, TX
UNIV OF TEXAS / TASSOULAS, AUSTIN, TX
UNIV OF WASHINGTON / MATTOCK, SEATTLE, WA
UNIV OF WISCONSIN / MILWAUKEE, WI
UNIV OF WYOMING / CIVIL ENGRG DEPT, LARAMIE, WY

USA BELVOIR / FORT BELVOIR, VA
USACOE / BRADLEY, VICKSBURG, MS
VA POLY INST AND STATE UNIV / MITCHELL, BLACKSBURG, VA
VIRGINIA INST OF MARINE SCI / GLOUCESTER POINT, VA
WEIDLINGER ASSOCIATES / LEVINE, LOS ALTOS, CA
WEST VIRGINIA UNIV / BARBERO, MORGANTOWN, WV
WEST VIRGINIA UNIV / KIGER, MORGANTOWN, WV
WOODS HOLE OCEANOGRAPHIC / LIB, WOODS HOLE, MA
WOODWARD CLYDE CONSULTANTS / OAKLAND, CA
WORCHESTER POLYTECH / SULLIVAN, WORCESTER, MA